REVIEW ARTICLE

Landslide susceptibility mapping along the China Pakistan Economic Corridor (CPEC) route using multi-criteria decision-making method

Ahsen Maqsoom[1] · Bilal Aslam[2] · Umer Khalil[1] · Zaheer Abbas Kazmi[3] · Sheheryar Azam[1] · Tahir Mehmood[1] · Ahsan Nawaz[4]

Abstract

This study maps the landslide susceptibility along the China–Pakistan Economic Corridor (CPEC) route using multiple landslide causative factors. A decisive statistical approach and the Geographic Information System (GIS) were used to map the route's susceptibility. The study area comprises a 236 km section of the Karakoram Highway, located in a region subjected to repeated landslides. The maps of different causative factors, including topographical, geological, and hydrological factors, were generated through GIS using data obtained from various sources. The causative factors were weighted according to their potential for developing a landslide event in a pairwise matrix of a multi-criteria decision-making approach. The analytical hierarchy process was applied to get the Consistency Index that governed the whole rating process. The weights of the landslide causative factors were used for generating the study area's final landslide susceptibility map. The results indicated that about 38% of the study area falls under the category of high and very high susceptibility. The outcomes of this study could be valuable in the identification of the parameters at a given area or region that are more prominently influencing the happening of landslides, in this way permitting the more viable preventive measures to be taken.

Keywords Landslide susceptibility · CPEC route · GIS · Analytical hierarchy process

Introduction

Natural hazards like slope failure, flood, and soil erosion have been caused due to the wrecking of a specific location's natural environment. Natural hazards are devastating occurrences with hydrological, geological, and atmospheric origins that can trigger casualties, devastate infrastructure, and upset social operations (Xu et al. 2016; Shahri et al. 2019). The substantial damaging influences on the atmosphere and society caused by landslides have introduced them to the world as significant natural hazards (Samia et al. 2017; Froude and Petley 2018; Cui et al. 2019). Considering the aftermath impact of disasters, it could be easily deduced that landslides rank among the top disasters with very severe consequences on human lives, local communities, economies, and the environment (Feizizadeh and Blaschke 2011). Studies have revealed that the landslides occurrence has amplified with the changing global climate and the growing concentration of human action (Apurv et al. 2015), particularly in rapidly evolving Asian countries (Kirschbaum et al. 2015). From 2004 to 2016, over 4800 severe landslide events had been recorded worldwide, leading to the loss of 56,000 lives, with over 300 million people internally displaced while nearly 3.7×10^6 km^2 of land devastated (Froude and Petley 2018). This has provoked investigators as well as knowledgeable associations to pursue effective responses to the prospective consequences (Nascimento and Alencar 2016).

Pakistan has been affected repeatedly by multiple natural disasters, including landslides. As a matter of fact, landslides are an underrated problem in Pakistan due to their unexpected nature. Unfortunately, the northern areas

✉ Umer Khalil
  umerkhalil745@gmail.com

1 Department of Civil Engineering, COMSATS University Islamabad Wah Campus, Wah Cantt, Pakistan

2 Department of Earth Sciences, Quaid-i-Azam University, Islamabad 45320, Pakistan

3 Department of Civil & Construction Engineering, College of Engineering, Imam Abdulrahman Bin Faisal University, Dammam, Saudi Arabia

4 Institute of Construction Project Management, CCEA, Zhejiang University, Hangzhou, China

of Pakistan have topographically active terrains that are prone to landslides, and no proactive measures are taken into consideration, which makes the situation even worse. The northern areas of Pakistan are linked with Western China through an important route known as Karakoram Highway (KKH). With the progress of the China Pakistan Economic Corridor (CPEC), of which KKH is the starting route in Pakistan, the future trade economy of both China and Pakistan will be revolutionized. Remarkably, the vertical gradient, earthquake sources, seismic regions, and extreme rainfall make the area along KKH more inclined to a natural disaster like landslides.

The Himalaya and Karakoram regions are topographically and seismically susceptible to landslides. Besides, the large volume of annual rainfall and the erosive nature of the land surfaces also make these regions vulnerable regions to landslides (Kanwal et al. 2017). The Attabad rockslide incident that occurred on 4th January 2010 triggered a death toll of 19 people, displaced 6000 people, and choked the Hunza river for 5 months. Consequently, this blockage resulted in immersing the 19 km part of the KKH, making a lake that still exists (Khan et al. 2019).

The mapping of landslide susceptibility is the spatial prediction of the incidence of a landslide by deliberating the roots of earlier incidents (Guzzetti et al. 1999). It is greatly dependent on the controlling factors and knowledge of slope movement (Yalcin 2008). Many researchers have formerly performed landslide susceptibility mapping studies to establish potential landslide hazard zones by assessing several controlling factors (Yalcin 2008; Shahabi and Hashim 2015; Basharat et al. 2016; Kanwal et al. 2017; Ali et al. 2019).

In recent times recently, the geographical information system (GIS) technology has been broadly utilized to assess landslide susceptibility (Mondal and Maiti 2013; Park et al. 2013; Paulín et al. 2013; Sujatha et al. 2014; Shahabi et al. 2015; Wang et al. 2016). Due to the GIS technology, it now has become possible to formulate and attain various thematic layers associated with the factors accountable for landslides in a given region (Shahabi et al. 2015). GIS tools have considerably enhanced the process in landslide susceptibility mapping in terms of both accuracy and efficiency (Weirich and Blesius 2007; Yan et al. 2019).

Khan et al. (2019) developed a landslide inventory based on remote sensing data and analyzed their spatial distribution for developing the landslide susceptibility map for the northern part of Pakistan (the Bagrote valley, Haramosh valley, and some portions of Nagar valley) using the frequency ratio method. Kanwal et al. (2017) used GIS-based datasets and techniques to map landslide susceptibility in the rugged mountainous terrain of Shigar and Shyok Basins situated in the Karakorum mountainous range in northern areas of Pakistan. Ali et al. (2019) used different geological and geomorphological factors to evaluate landslide susceptibility along the KKH route using the analytical hierarchy process (AHP).

Implementing proper planning and development policies in reducing landslide's disaster can assist in minimizing impending threats of a landslide, but this requires a comprehensive evaluation of this under-estimated peril (Calligaris et al. 2013; Ahmed et al. 2014). Thus, mapping of landslide susceptibility is a crucial step preceding landslide evaluation, planning, managing, and disaster mitigation. Various criteria could be considered while evaluating a spatial problem (Ray and De Smedt 2009; Oh and Pradhan 2011). These criteria can be greatly influenced by the investigator's value judgment and ambiguity (Ahmed et al. 2014). To overcome the improper decision making and the uncertainty associated with the problem, multi-criteria decision-making methodology (AHP) has been applied in this investigation. AHP is a flexible and straightforward technique to evaluate and resolve intricate issues (Saaty 1987, 1990). It expedites the valuation of the possible influence of various factors on landslide development by comparing them in possible pairs in a matrix (Ali et al. 2019). The formerly conducted studies have considered multi-criteria decision-making a better choice due to its precision in predicting landslide potential (Kamp et al. 2008; Pourghasemi et al. 2012; Park et al. 2013; Ahmed 2015; Basharat et al. 2016).

This region has huge importance due to the CPEC route. Since this region has complex geological structures, receives a high amount of monsoon rainfall, and has rapid urban changes, there is a dire need to develop the fundamental model to map the landslide potential areas in the region. Also, this study provides a baseline for other complex regions to map the landslide potential areas using multiple causative factors.

The present study aims to produce a landslide susceptibility map of the intended area using GIS and remote sensing. A hierarchy of causative factors is constructed in AHP. Afterward, comparisons were made among probable pairs in a matrix to assign a weight for each factor, and ultimately the Consistency Ratio was computed. This assigning of weights to causative factors helped to demonstrate linguistically framed and personally assumed knowledge in mathematical ways. In making the CPEC route more feasible and safer, the policymakers can provide possible provisions using produced landslide susceptibility map. Moreover, the findings of this study can be effectively used for future landslide mitigation projects and the ongoing infrastructure works within the considered area (Gilgit to Bara Khun).

Study area

Northern Pakistan is connected to Western China through the Karakoram Highway (KKH), which is undergoing rehabilitation and improvement under the revolutionary initiative

of CPEC. The KKH passes through the mountainous areas of Karakoram, Hindukush, and the Himalayan Mountain range that joins Indian and Eurasian tectonic plates, including Kohistan Island Arc (Ding et al. 2018). The area under investigation is a 236 km (10 km buffer) section of KKH, running from Gilgit to Bara Khun. Gilgit is the starting point of the study area and is the capital city of region Gilgit-Baltistan, situated in northern Pakistan (Fig. 1). Due to its geostrategic significance to the silk route, the ancient town of Gilgit, having geographical coordinates 35.8819° N, 74.4643° E, has been an important trading hub for ages. The other end of the study area having geographical coordinates 36.8761° N, 75.1622° E is Bara Khun. The study area has diverse lithologies (igneous, metamorphic, and sedimentary), seismic hazard zones, high reliefs, subterranean crevices, arid to monsoon climate, cracked and endured rock masses, and locally high rates of tectonic activity. The area

under investigation becomes a unique geohazard laboratory because of these geological, lithological, and weather conditions (Ali et al. 2019). The diversity of the geohazards in the region has remained a significant source of concern to KKH's stability since 1979 (Ali et al. 2019). Rakaposhi and Nanga Parbat, with elevations of 7788 and 8126 m, respectively, are among the world's most significant summits in this area (Hewitt 1998). Previous studies reported that the study area is among the steepest places on earth, where there is sudden descent in elevation from 7788 to 2000 m within the proximity of 10 km (Goudie et al. 1984).

Uncertainty in the weather conditions along the KKH is being observed due to immense change in yearly average gradient (− 5 to 46 °C) and shower (15 to 1500 mm). During the westerlies (January, February, and March) and the prevailing seasonal winds (July, August), a colossal rainfall occurs in the study area. Moreover, in the Hunza valley

Fig. 1 Map of the study area showing the location of the area in Pakistan and the elevation of the area
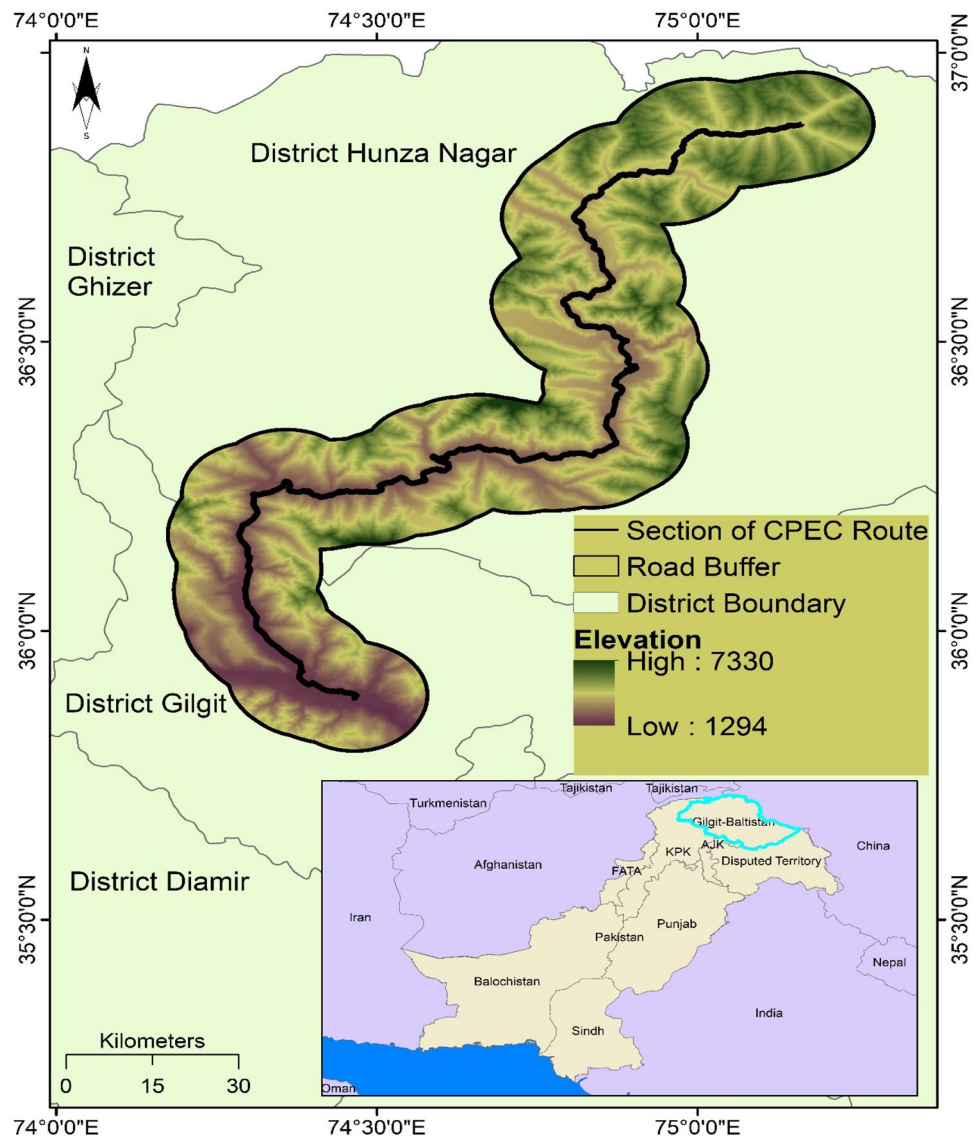
region, situated along the KKH, the vertical climatic zonation exists. Semi-barren to barren weather conditions categorize the valley floor, but precipitation greater than 1000 mm is received by adjacent summits and slopes higher than 5000 m (Hewitt 1998). A portion of the world's long mainland glaciers with the most elevated icy disintegration and the steepest angle falls in Karakoram and Himalaya (Goudie et al. 1984). Within the vicinity of KKH, there are noses of numerous icy cliffs such as Batura, Ghulkin, Pasu, and Gulmit. Moderately warm temperatures in the valleys are the reasons behind the unexpected melting of ice, resulting in regular flows, disastrous debris flows, blockage. From the commencement of the Indo–Eurasian collision 50 Myr ago, the orogenic features that the area is composed of started forming. and stream The active faulting, subduction, and cluster shortening still ongoing in the region are due to elevated rates of ~ 7 mm per year (Zeitler 1985) and merging rates of 4–5 cm per year (Jade et al. 2004). Significant earthshattering characteristics along the highway responsible for brittle distortion include Raikot Fault, Kamila Jal shear zone (KJSZ), Karakoram Fault, Main Karakoram thrust (MKT), and Main mantle thrust (MMT) (Goudie et al. 1984; DiPietro and Pogue 2004). Brittle distortion thus results in immense articulation and cracking of rock mass.

Materials and methods

Landslide inventory mapping

Landslide distribution is associated with the conditioning factors, and that association is revealed by landslide inventory mapping (Pourghasemi et al. 2012). Several investigators made landslide inventory maps through airborne photographs and satellite images (Pradhan and Lee 2009; Pradhan et al. 2010; Suh et al. 2011; Umar et al. 2014). The areal distribution of existing landslide areas is shown by landslide inventory (Cevik and Topal 2003). The landslide locations need to be located accurately for the probabilistic landslide susceptibility analysis. Field survey of the area, aerial photographs, and interpretations worked out earlier, and the data extracted from past and present landslide distribution provide a supportive platform for preparing the landslide inventory map (Van Westen et al. 2006).

To formulate a multi-temporal landslide inventory along the highway, we utilized constant information of landslide happenings extracted from the Geological Survey of Pakistan (GSP) journals, an examination article (Hewitt 1998), and Google Earth imagery as well as GIS imagery. The degree of importance of each landslide causative factor was realized by incorporating a landslide susceptibility map created by the distribution maps of causative factors with the prepared landslide inventory map.

Important landslide causative factors and their selection

For landslide susceptibility mapping, evaluation of the factors triggering landslides is critical. Susceptibility maps have been prepared by most of the domestic and foreign researchers who have investigated numerous landslides triggering factors. The selection of landslide causative factors stems from the landslide occurrence in a specific area and data availability (Lee and Min 2001). For investigations to proceed using GIS, the considered factors must be comprehensive, uneven, functioning, computable, and essential (Ayalew et al. 2005). Landslide causative factors that are generally considered include geographical, morphological, seismo-earthshaking, and climatic factors (Kamp et al. 2008). In the present study, a landslide susceptibility map is prepared by considering the succeeding 13 causative factors: elevation, slope, lithology, rainfall, drainage intensity, Normalized Difference Water Index (NDWI), structural fault, landuse, earthquake hazard, Normalized Difference Vegetation Index (NDVI), aspect, soil type, and plan curvature.

The soil type is a vital landslide causative factor. The strength of the soil is significantly decreased by an increase in pore water pressure caused by the rainwater infiltration, which causes landslides (Sidle and Ochiai 2006; Yan et al. 2019). The slope comprises a certain lithology, which plays a vital role in the initiation and pattern of failure. Since each lithology has its peculiar way of behaving to the stresses, the susceptibility of a slope to failure can be related to its lithology (Ali et al. 2019). As reported in many previous studies (Pourghasemi et al. 2012; Mondal and Maiti 2013; Chen et al. 2016; Wang et al. 2016), lithological features need to be considered as controlling factors in developing landslide susceptibility maps. As the considered region has a mountainous terrain and the geology is composed of rocks and soil, and they contribute in their own peculiar ways to trigger landslides, it becomes important to consider both factors.

The degree of a slope plays an unswerving role in the initiation of landslides and is considered a foremost factor in slope stability analysis (Lee and Min 2001). While preparing the landslide inventory maps, the degree of the slope is used as a triggering factor all the time (Ercanoglu and Gokceoglu 2004). Landslides initiated by the rainfalls have been the subject matter for many researchers in the past (Alimohammadlou et al. 2014; Schilirò et al. 2016).

The drainage proximity should also be given due weightage in determining the stability of a slope (Akgun et al. 2008; Wang et al. 2015; Basharat et al. 2016; Demir 2019). The stability of the slope is badly affected by the tributaries, which erode the adjacent slopes and increase the water level by drenching the bottom of the slope mass (Pourghasemi et al. 2012; Ali et al. 2019). Previous studies have proven distance to stream as a governing aspect of slope stability

(Pourghasemi et al. 2012; Chen et al. 2016; Moosavi and Niazi 2016; Hong et al. 2018). The degree of saturation of the slope material is a vital regulating parameter for slope stability (Yalcin 2008). Rivers flowing along the slopes erode their toes and saturate their lower parts (Yan et al. 2019). An escalation in the total wetness index considerably increases the possibility of triggering the landslide (Kanwal et al. 2017).

On the contrary, the distance of slope from major thrusts and faults also affects the strength of the rocks and soil permeability, thus monitoring landslide susceptibility. The stability of a slope is greatly affected by lithology containing faults, folds, joints, and fractures (Yan et al. 2019). Many researchers in the past, while undertaking landslide studies, employed distance to fault (Pourghasemi et al. 2012; Moosavi and Niazi 2016; Wang et al. 2016; Hong et al. 2017; Pradhan et al. 2017). While conducting studies on causative factors for landslides, many professionals considered earthquakes vital (Refice and Capolongo 2002; Yan et al. 2019). Many earthquakes in the study area are caused by the presence of vertical (or nearly vertical) fractures and active thrusts, presently causing frequent landslides (Ali et al. 2019). Although faults play an essential role in triggering earthquakes, the purpose of considering both earthquakes and faults is that the slopes in the vicinity of faults appear to be weaker due to the triggered earthquakes, and the earthquake is a regional phenomenon. Considering the topographic and geological characteristics of the region, it is essential to consider both these factors.

Variation in land use affects the hydrological state of the slopes and consequently makes the slopes unstable. Different types of land use have their particular role in the stability of slopes like soil erosion is resisted by vegetation. In contrast, plain rock or soil increases slope susceptibility to failure (Reichenbach et al. 2014). There is a strong relationship between land use and landslide events, as observed by Restrepo and Alvarez (2006).

The high concentration of vegetation keeps the slopes more intact and less prone to landslides. The slope stability is directly mirrored by NDVI that reveals the portion of the area covered with vegetation (Cevik and Topal 2003; Demir 2019). Landslide occurrence is greatly influenced by NDVI (Shahabi et al. 2012). NDWI reveals areas with high surface moisture; thus, it is an indirect indication that these areas have high groundwater potential. As landslide is predominantly affected by surface moisture, it is important to consider its impact. Areas having higher surface moisture are more susceptible to landslides. The effective reasons like soil moisture, sunlight, and wind due to aspects, experienced by the slopes affect the stability of slopes (Dehnavi et al. 2015). Many researchers also regard slope curvature as a significant topographic aspect for causing landslides (Greco et al. 2007; Mandal and Mandal 2018).

Methodology

First, all the selected landslide causative factors were obtained from different data sources and then were calculated to prepare the thematic maps in GIS. The details about the data sources and calculations are discussed in the next section. The factors were then arranged in a pairwise matrix for the computation of their relative importance through AHP. After that, the factors were incorporated in the GIS environment by multiplying the calculated weights with the factors through the weighted overlay to produce the final susceptibility map. The final susceptibility map was divided into five susceptibility classes using the natural break method. The landslide inventory was used to check the accuracy of the map. Past landslide locations from the inventory were marked in the final susceptibility map to demonstrate its accuracy. The detailed methodology is presented in Fig. 2.

Structuring of thematic maps

In organizing the thematic maps of slope, aspect, elevation, and curvature, a natural break procedure is used in GIS. Through the process of interpolation of annual rainfall data extracted from satellite, the precipitation map was formed. For the present study, the rainfall data from Global Precipitation Measurement (GPM) was utilized. This satellite is the product of the National Aeronautics and Space Administration (NASA). It is extensively utilized because of the enhanced accuracy of the data. The land use data of the Food and Agricultural Organization (FAO) was used to obtain the land use of the study area. The Landsat 8 satellite data was used for the thematic maps of NDVI and NDWI. The NDVI and NDWI data were collected for a year, and then the average values were calculated for the whole study area. The factors were calculated using the techniques presented in Table 1.

Drainage density was extracted using the Shuttle Radar Topography Mission (SRTM) based digital elevation model (DEM) from Arc Hydro tools. The DEM was also used to structure the thematic layers of topographical features: elevation, aspect, slope, and plan curvature. The obtained DEM was of 30 m × 30 m resolution. Therefore, all the remaining thematic maps that were obtained from other sources were also resampled to 30 m × 30 m resolution. Previously published geological and seismic maps helped in digitizing the maps of structural faults, lithology, and earthquake hazard. The geological data of the study area obtained from the Geological Survey of Pakistan also helped in the preparation of the soil type. All the factors were classified into different classes using the natural breaks method.
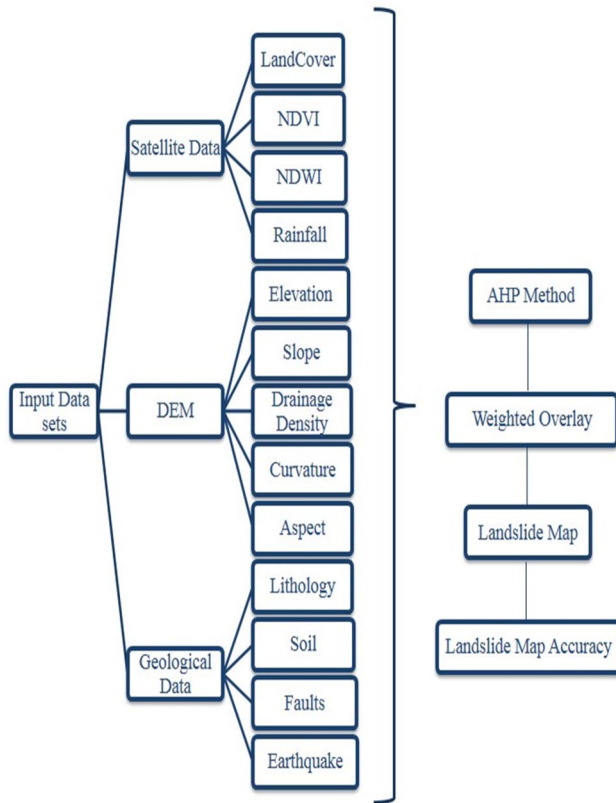
Fig. 2 Detailed methodology

Analytical hierarchy process (AHP)

Saaty ([1990](#)) introduced the analytical hierarchy process (AHP) to address the decision-making in assorted-program

and diverse-objective matters. A framework-based pairwise judgment based on the role of various variables is made using AHP as indicated by the professional's decisions (Saaty [2008](#)). If the paring y-axis parameter is less significant than the x-axis parameter, the assigned value will be between 1 and 9. In contrast, if the y-axis factor is a more prominent triggering factor, then the given value will be in reciprocals ranging from 1/2 to 1/9, as suggested by Saaty ([1987](#)).

Consistency ratio (CR) is used to assess the process and avoid discrepancies in assigning specific scores to regulatory parameters in a just and impartial manner (Basharat et al. [2016](#); Kanwal et al. [2017](#); Pourghasemi and Rossi [2017](#); Ali et al. [2019](#)). After investigating 500 samples, Saaty ([1987](#)) shaped the table (Table [2](#)) of the Random Consistency Index (RI). CR is then computed by comparing RI from the table and CI from calculations, as shown in the following equation:

$$CR = \frac{CI}{RI}. \tag{1}$$

In the above equation, CR is the Consistency Ratio, CI is Consistency Index, and RI is a Random Index. The value of RI is already established for different numbers of parameters, while the following equation was used to calculate the value of CI:

$$CI = \frac{(\lambda_{max} - n)}{n - 1}. \tag{2}$$

In the above equation, λ_{max} is the extreme eigenvalue obtained during the AHP process, and n indicates several

Table 1 Sources and used techniques for calculating the factors

Parameter	Source	Technique/formula	References
Elevation	STRM DEM	30×30 m DEM	Saha et al. ([2019](#))
Slope	STRM DEM	$\tan \theta = \frac{N \times i}{636.6}$ $N =$ no. of contour cutting; $i =$ contour interval	Wentworth ([1930](#))
Aspect	STRM DEM	$R(p,q) = 1 - \sqrt{2}\left(\frac{b}{K\delta}\right)\sqrt{1 + q + q^2}/(1 - p + q)$	Horn ([1981](#))
Plan curvature	STRM DEM	$K = \left\|\frac{dT}{ds}\right\|$	Zevenbergen and Thorne ([1987](#))
Drainage density	STRM DEM	Proximity analysis	Pavelsky and Smith ([2008](#))
Rainfall	PMD	$R = \sum_{i=1}^{12} 1.73x_{10}\left[1.5 \log_{10}\left(p_i^2/p\right) - 0.08188\right]$	Arnoldus ([1980](#))
Landuse	FAO landuse	Maximum likelihood	Anderson ([1971](#))
NDVI	Landsat-8	$\frac{NIRBAND - IRBAND}{NIRBAND + IRBAND}$	Carlson and Ripley ([1997](#))
NDWI	Landsat-8	$\frac{Green - NIR}{Green + NIR}$	Ekumah et al. ([2020](#))
Structural faults	Geological map of Pakistan	Proximity analysis	Pavelsky and Smith ([2008](#))
Earthquake hazard	Seismic map of Pakistan	Proximity analysis	Pavelsky and Smith ([2008](#))
Soil data	Geological map of Pakistan	Proximity analysis	Pavelsky and Smith ([2008](#))
Lithology	Geological map of Pakistan	Proximity analysis	Pavelsky and Smith ([2008](#))

Table 2 Pairwise comparison of datasets

Causative factors	Soil type	Slope	Rainfall	NDWI	NDVI	Lithology	Landuse	Structural fault	Elevation	Earthquake hazard	Drainage density	Plan curvature	Aspect
Soil type	1	2	2	3	4	3	3	2	7	5	6	7	7
Slope	1/2	1	3	2	3	4	4	2	8	5	6	9	9
Rainfall	1/2	1/3	1	5	5	3	4	2	7	6	7	9	9
NDWI	1/3	1/2	1/5	1	2	6	4	2	4	3	4	7	7
NDVI	1/4	1/3	1/5	1/2	1	2	3	2	4	2	3	7	6
Lithology	1/3	1/4	1/3	1/6	1/2	1	3	2	5	2	3	6	6
Landuse	1/3	1/4	1/4	1/4	1/3	1/3	1	2	3	2	2	5	5
Structural fault	1/2	1/2	1/2	1/2	1/2	1/2	1/2	1	7	6	7	8	9
Elevation	1/7	1/8	1/7	1/4	1/4	1/5	1/3	1/7	1	2	2	3	3
Earthquake hazard	1/5	1/5	1/6	1/3	1/2	1/2	1/2	1/6	1/2	1	2	5	5
Drainage density	1/6	1/6	1/7	1/4	1/3	1/3	1/2	1/7	1/2	1/2	1	5	5
Plan curvature	1/7	1/9	1/9	1/7	1/7	1/6	1/5	1/8	1/3	1/5	1/5	1	1
Aspect	1/7	1/9	1/9	1/7	1/6	1/6	1/5	1/9	1/3	1/5	1/5	1	1
Weight	4.55	5.88	8.15	13.54	17.73	21.2	24.23	15.68	47.66	34.9	43.4	73	73

causative factors considered (Guo et al. 2017). The value of CR indicates variation in the professional's decision during the evaluation of the parameters. The decisions during the assessment of parameters were considered unbiased if the CR value is lower than 0.1, while values greater than 0.1 shows discrepancies and propose a revised decision.

Causative factor weight distribution using AHP

Based on studies previously conducted, individual opinions of experts, nature, and physical properties of parameters helped in determining the encumbrance of causative factors using AHP (Calligaris et al. 2013; Basharat et al. 2016; Wu et al. 2016; Kanwal et al. 2017; Ali et al. 2019; Demir 2019; Khan et al. 2019). Satty's suggested numerical scale was used as a source for these values, which were allocated analytically using the AHP method.

Results

Thematic maps of causative factors

The elevation of the study area varies from 1294 to 7330 m (Fig. 1). The targeted area was divided into five classes concerning its elevation (1294–2336, 2336–3171, 3171–3939, 3939–4727, and 4727–7330 m). Most of the study area has high altitude. As evident from the extracted map, the north-eastern portion (Bara Khun and Sharhkater) has concentrated high-elevation slopes. On the contrary, the prominent city of Gilgit and the nearby areas have the lowest elevations among the rest of the considered region. The soil in the study area is mainly categorized as clay, loam sand, sandy clay, and silt (Fig. 3a). The slope map of the area was divided into five classes having a recess of 15 degrees in the slope. The degree of slope for the whole study area ranges from $< 15°$ to $> 60°$ consisting of most slopes between 30° and 45° (Fig. 3b). On the contrary, the study area has scattered steeper slopes ($> 60°$). The KKH passes through the region having diverse lithologies, including the three most common sedimentary, igneous, and metamorphic. The lithology of the region is divided into five classes (Fig. 3c). The Chalt, Gulmat, Baltit, Nagar, Atabad areas, situated along the highway, are entirely composed of metamorphic and volcanic rocks, while the Bara Khun area is composed of soil solely.

The study area has been divided into five classes to locate high and low annual rainfall areas. The map (Fig. 3d) depicts that the Normal and Chalt regions experience the most increased annual precipitation (11.62 to 11.81 mm). At the same time, most of the study area is predominantly subjected to moderate to high annual rainfall (11.33–11.62 mm). A detailed drainage density map is shown in Fig. 4a. Many small tributaries feed two main rivers in the region (Indus
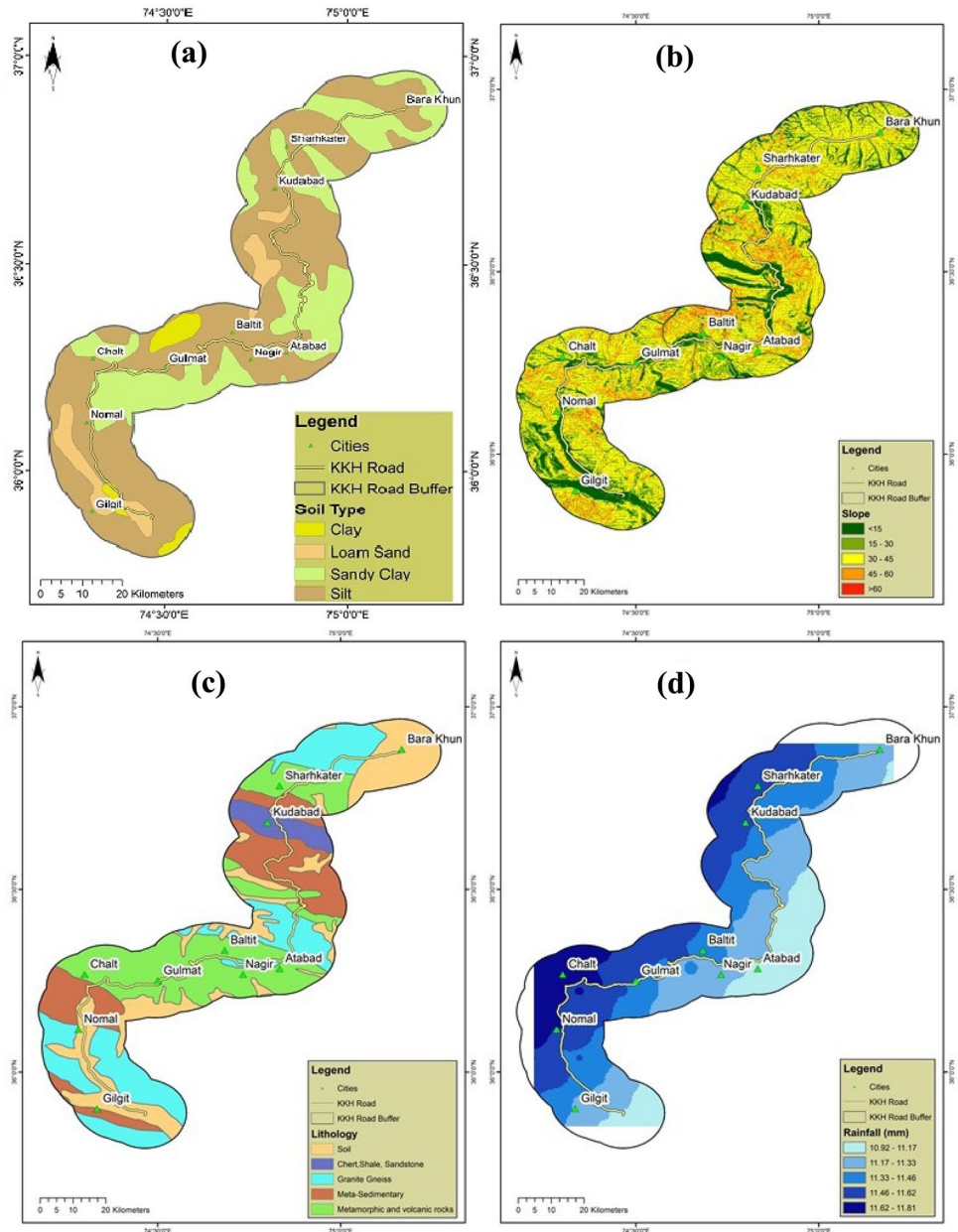
and Hunza). Due to the hilly terrain and frequent rainfalls and snowmelt, the area is home to ample drainage tributaries of different notches, as evident from the map. These watercourses carrying mud, debris, and large discharges display high-energy flows after substantial rainfalls during the monsoon season. The regions where the drainages value is high having the highest landslide potential as the moisture content in these regions is high. Higher moisture content decreases soil strength.

The NDWI details for the study area are presented in Fig. 4b. High NDWI values have been observed for the study area with higher elevation. The northwestern and somewhat the central portion exhibits high wetness index. The remaining part of the exploratory area shows a low wetness index.

The regions with high wetness index are more prone to landslide than those with a low wetness index. High wetness decreases soil strength as wet soil becomes loose and is more prone to landslide. Within the proximity to the KKH, the significant structural features are Hispar Fault, Khudabad Fault, and the Main Karakoram Thrust (MKT). The fault layout for the study area is shown in Fig. 4c. Based on the published mountainous region classifications for land use, the study area is categorized into agriculture in the valley, bare areas, natural herbaceous, high natural shrubs, snow, and water bodies (Fig. 4d). Nearly half of the study area is represented by natural herbaceous. The second most prominent land use category is snow. The region is in the extreme north of Pakistan and is a highly elevated mountainous region. It receives

Fig. 4 **a** Drainages, **b** NDWI, **c** structural fault, **d** land use data of the study area
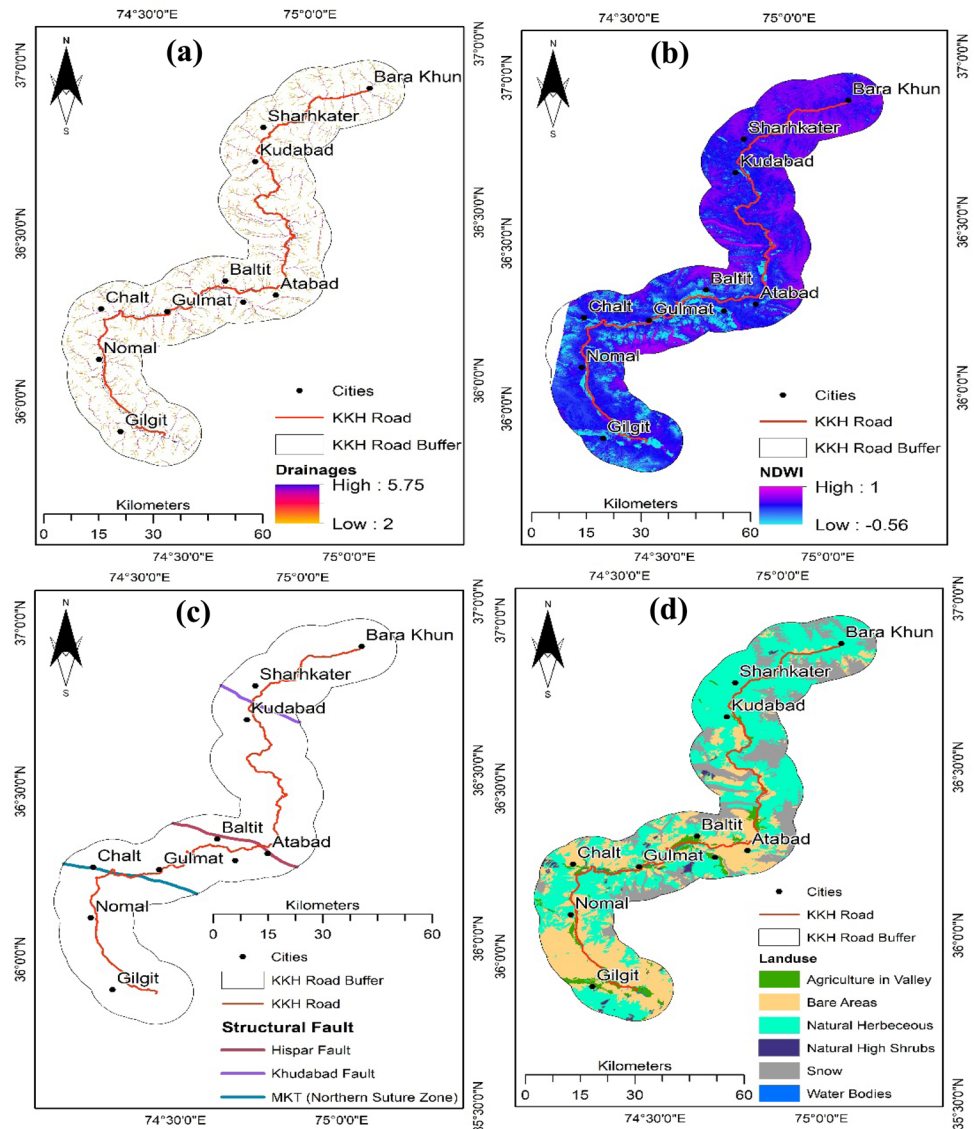
substantial snowfall during the winter season that keeps covering the most elevated parts of the area throughout the year.

The earthquake hazard map is prepared based on landslide density caused by seismic events in the past (Fig. 5a). The considered region is sorted into three different categories regarding earthquake hazards as moderate, high, and very high. NDVI distribution visualization of the area under study has been prepared through the raster calculation tool in ArcGIS. A low value of NDVI for almost the whole central and northeastern portion of the study area is observed. The southeastern and, to some extent, the central part represents the high vegetation cover, as illustrated in Fig. 5b.

The aspect map is divided into the following ten divisions: flat, north, northeast, east, southeast, south, southwest, west, northwest, and north. All these aspect classes are scattered all over the area, as can be seen from Fig. 5c. The more prominent aspect classes are north, south, and

southwest. By taking the second derivative of the DEM, a curvature map was prepared for the whole study area containing the concave and convex classes. A positive curvature value represents the convex slope, and a negative curvature value represents a concave slope. Most of the study area has an intermediate curvature, as evident from Fig. 5d.

The relative importance of causative factors

As mentioned earlier, all the parameters were assigned the values, as shown in Table 2, considering their importance in a pairwise comparison. The primary purpose of this rating process was to have a weightage of each landslide conditioning factor, which can further help assess the landslide susceptibility of the study area. The weightage of each parameter is shown in Table 3, which depicts that soil type (17%), slope (16%), rainfall (16%), and NDWI (11%) were found to

Fig. 5 **a** Earthquake hazard, **b** NDVI, **c** aspect, **d** plan curvature of the study area
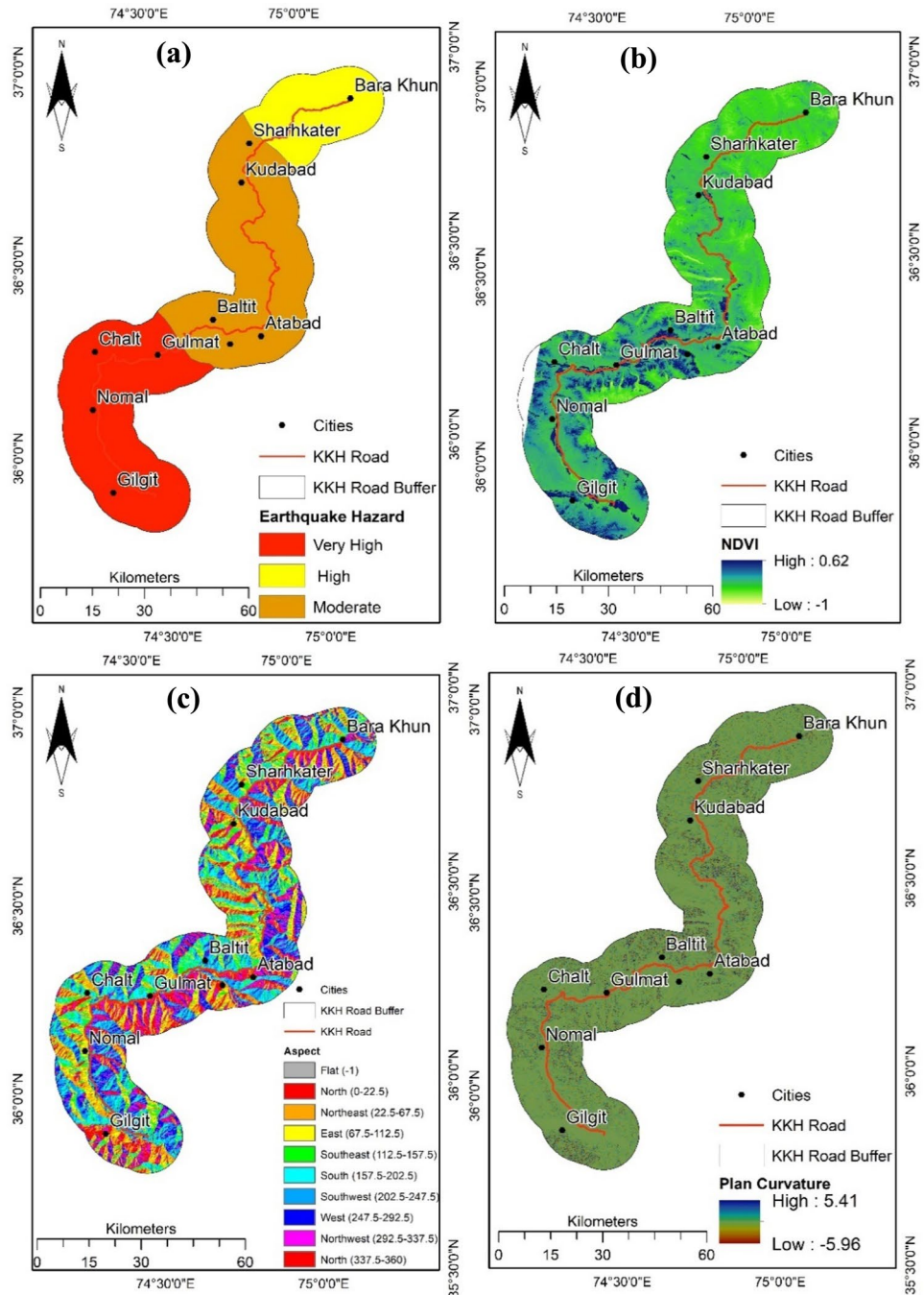
be more prominent conditioning factors. In the study area, these mentioned parameters are more causative factors and can trigger a landslide.

Landslide susceptibility map

There were five main susceptibility classes in the produced landslide susceptibility map comprising very low, low, moderate, high, and very high susceptibility, as illustrated in Fig. 6a. Those regions which mainly receive higher rainfall

have a vertical gradient, weaker lithologies, and high NDWI are under very high susceptibility.

The region of the study area along the KKH from Gulmat to Kudabad has high and very high susceptibility than the other region, as evident from the map. Specifically, the region near the city of Baltit is an active landslide zone. The regions near the city of Gilgit and Bara Khun have very few slopes that are highly prone to failure. Thus, it can be concluded that these regions along the KKH are under modest to high susceptibility. The percentages of the area in different

Table 3 Computed weights for each dataset

Sr. no	Dataset	Weightage (%)
1	Soil type	17
2	Slope	16
3	Rainfall	16
4	NDWI	11
5	NDVI	7
6	Lithology	7
7	Landuse	5
8	Structural fault	9
9	Elevation	3
10	Earthquake hazard	3
11	Drainages	3
12	Plan curvature	1
13	Aspect	1

Table 4 The area under different susceptibility classes

Classes	Area (%)
Very high susceptibility	16
High susceptibility	22
Intermediate susceptibility	34
Low susceptibility	13
Very low susceptibility	15

In total, 22 landslides were randomly identified from the past using satellite data, out of which 19 lies in high or very high susceptibility zone. In contrast, only 3 lie in the low susceptibility zone. Consequently, it can be justified that the model build for the intended purpose gives relatively better accuracy.

hazard zones are listed in Table 4. It shows that about 38% of the study area is subjected to sufficiently high susceptibility, whereas only 15% is subjected to very low susceptibility.

Accuracy assessment

The accuracy of the landslide susceptibility map was analyzed from the point dataset of the past landslides. These landslides were taken from the Landsat 8 satellite data (Fig. 6b). It shows that the accuracy of the map is 86%, which means that the model built in this study is acceptable.

Discussion

Before working on disaster mitigation and landslide valuation arrangements, the primary focus will be on landslide susceptibility mapping (Fell et al. 2008; Kanwal et al. 2017). The size of the area for which the study is to be conducted governs while selecting the method for susceptibility mapping and the accessibility of data it accounts for. The quality of results generated is greatly influenced by the superiority

Fig. 6 **a** Landslide susceptibility map, **b** accuracy assessment of the map
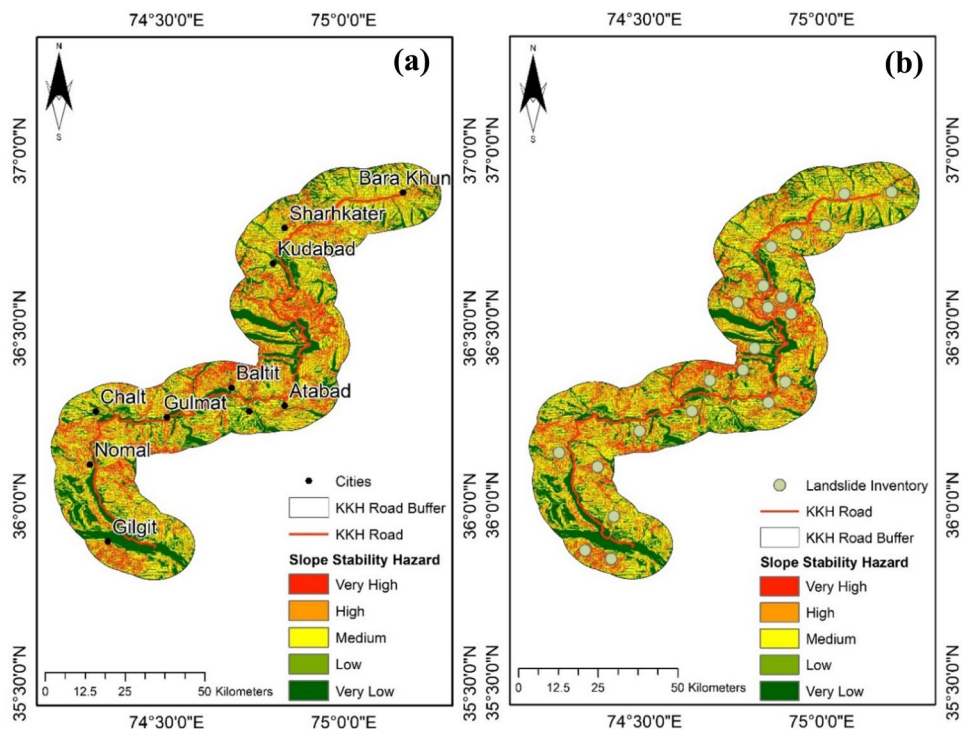
of datasets (Fressard et al. 2014). One of the most significant and fundamental datasets is landslide inventory. The accuracy of the final map is adversely influenced by the recent landslide activities and the imprecise judgment of the location. We used satellite imagery to prepare landslide inventory for this research. It is acknowledged that the landslide triggering factors in the past will account for future landslides because landslides do not occur that often. Hence, it is not possible to have the data for the whole area under investigation, which led to the use of the qualitative index-based experimental methodology in the GIS atmosphere to evaluate landslide susceptibility. For spatial mapping of the study area's landslide susceptibility, 13 causative factors (elevation, lithology, slope, NDVI, structural fault, aspect, earthquake hazard, drainage density, NDWI, soil type, rainfall, land use, and plan curvature) were selected based on the literature review and the characteristics of the study area. The satellite data of Landsat 8 was used for land use, NDWI, NDVI, while DEM was used for elevation, slope, aspect, curvature, and drainage density. There are different rating values assigned to each parameter, having a range between 1 and 9 inclusively, where 1 indicates that the parameter is less causative and 9 being the most. Each class has a rating value, which are the results of studies conducted previously and the opinions of experts (Calligaris et al. 2013; Ahmed et al. 2014; Kanwal et al. 2017).

The weights of all the datasets obtained by exploiting AHP are given in Table 3. The guaranteed approach to get more reliable results is the use of the qualitative and decisive approach. The detailed study of causative factors showed that more landslides have occurred in regions of weak lithologies, high NDVI, high rainfall, and steeper slopes. It has also been noted that with the increase in distance from faults and drainage tributaries, the potential of landslide occurrence decreases, as evident from the maps.

The rainfall intensity along the KKH is highly fluctuating throughout the year, with average precipitation ranging from 15 to 1500 mm. Depending on the forebear soil moisture, hill slope, and many other factors, different rainfall intensities could be enough to trigger the landslides. For example, a saturated piece of soil on a slope might just need a small amount of water enough to trigger the landslide. The most projecting soil category for the study area is silt, followed by sandy clay, loam sand, and clay. The rainwater, which infiltrates in the soil mass, acts as a facilitator by adding to the weight of a slope, making it softer, increasing the pore hydro force, reducing the frictional resistance, and reducing the shear strength of the soil. A convincing relation between precipitation and mass movement has been observed by different researchers within the proximity of the highway (Ali et al. 2019). In 1999, the KKH experienced enormous landslides, which lead to the blockage of traffic in the region. After the landslide events, the precipitation maps were overlapped with the landslide happenings, and a visible synchronization was found between the crests of mass movements and high precipitation months (Ali et al. 2019). Hefty precipitations and the winds from the west also generate landslides in the monsoon, so it is also regarded as an important factor. However, the effect diminishes in the north of Gilgit, where landslides are caused by the aggregate impact of ice melting with ascending temperature and rainfall. Moreover, among all the aspect classes, the slopes facing north are more vulnerable to landslides (Sidle and Ochiai 2006; Yan et al. 2019). Slopes facing south to the northwest are more susceptible due to the influence of significant southwest to the southeast azimuth of cyclical downpour rainfalls, as suggested by many other studies (Ahmed et al. 2014).

The more it acquaints with drainage concentration, slope volatility, and saturation as a slope section is incorporated by added positive and negative curvature value. The cohesive property of the soil is greatly influenced by soil saturation caused by water accumulation in the concaved slope. In comparison, regular expansion and contraction are tolerated by convex slope, the rocks break, and decay. Percolated water results in decayed and slackened material over the curving slope, which boosts pore water pressure leading to slope instability (Mandal and Mandal 2018). The pore water pressure in disconnected soil deposits rises after heavy precipitation during the monsoon, and the prevailing winds from the west activate many landslides.

In addition to these factors, the active faults and shear zones are important controlling parameters as most landslides gather around them. Hispar, Khudabad, and the MKT faults are the prominent structural features within the proximity of the KKH. The slopes are highly distorted along these active faults, and landslides are expected to occur (Ali et al. 2019). Highly fractured and jointed rock masses, which are incredibly susceptible to failure, result from these tectonic features. Since 1904, 317 earthquakes of magnitude greater than 5 while 10 earthquakes of magnitude greater than 7 jolted the region along KKH. It includes the October 2005 earthquake in Muzaffarabad ($M = 7.6$) and October 2015 earthquake in Afghanistan ($M = 7.5$) (Zhiquan et al. 2016; Ali et al. 2019). These seismic zones have created fractures and vents in rock masses. Rainfall penetrates the vents formed in rocks due to an earthquake, thus disturbing the stability of the rock mass and ultimately resulting in slope failure. Other geomorphological factors (elevation, aspect, curvature) were less connected with landslide events, so they were rated low. The closeness of road features to slopes might cause slope catastrophe leading to landslides due to the undercutting of the slopes. Slopes composed of sandstone, limestone, slates, and shales are more prone to failure.

Consequently, earthquake hazard and lithology are rated high but are fewer triggering factors than the slope. The slopes of weaker lithologies such as chert, shale, sandstone, and soil can quickly destabilize because of other happenings such as earthquakes and rainfall. Although the southern and northern parts of Gilgit city are defined as granite, which is the most durable rock structure of the region, these parts are shown as high susceptibility areas in the final map. The reason for this high susceptibility is that in the vicinity of the city, other essential factors such as the construction of roads and houses destabilize the slopes.

The focus of this work is based on the AHP technique to map the landslide susceptibility of the considered area. Previously, landslide susceptibility maps were organized by various researchers using the AHP model (Park et al. 2013; Ahmed 2015; Shahabi and Hashim 2015; Pourghasemi et al. 2016; Pourghasemi and Rossi 2017). For applying the AHP technique, all the causative factors were rated according to their importance, and then the landslide susceptibility map was developed using the weighted overlay method (Basharat et al. 2016; Ali et al. 2019). The ratings assigned to the causative factors for preparing a landslide susceptibility map of the study area represented a CR of 0.0931. This CR value less than 0.1 concludes that using AHP and bearing in mind the ranking value class, the weight allocated to each landslide causative factor was impartial. The critical established contributing factors include NDWI, rainfall, slope, and soil type.

The purpose of the research was the extraction of the data about the landslide causative factors and point out the factors causing landslide catastrophes. An information-driven strategy runs the module as its spine through affectability analysis can aid in examining several landslide causative factors. Using this research, public and private working agencies within the proximity of the study area can make decisions in fast identification of the vulnerable regions, support a far-reaching and changed examination of areas of choice, and back electing and dealing with an early notice framework.

Conclusions

This study created a landslide susceptibility map utilizing factual approaches, i.e., AHP and GIS. 13 causative factors, namely elevation, slope, lithology, earthquake hazard, rainfall, structural fault, aspect, plan curvature, land use, soil type, NDWI, NDVI, and drainage density were considered. Each one of the parameters was allocated a numerical weight using AHP. The relation between landslides and the contributing factors is analyzed by many of the qualitative and quantitative techniques. For cracking a multi-factor problem such as landslide occurrences, the AHP method holds importance. But, in identifying the comparative importance of these causative influences, assorted professionals have different ideas. The result and the efficiency of the result are reliant on the eminence of the provided data. The results can be improved and generated rapidly on-demand as the method used is very convenient. The KKH is characterized by a variety of mass wasting: rockfall, debris fall, rockslide, debris slide, debris flows, and mudflows. The increased number of activities on steep mountain slopes is mainly due to the increasing population pressure. The final landslide susceptibility map was divided into five different classes (Fig. 6a). The zones with a specific fraction of susceptibility, i.e., 16–22%, show that the slopes of these zones are significantly prone to landslide. Landslides being a heavy disaster event, not just cause sudden causalities but can cause damage to infrastructure, resources, and erotic life. Thus, the development of future construction projects and land use in similar areas can be proceeded appropriately by using susceptibility maps to shield social life and infrastructure from landslides. More detailed investigations and landslide prevention engineering solutions are required for the areas where the susceptibility is very high. If proper engineering prevention techniques are adopted, the threat to life and property can be significantly reduced. As proposed by the results, NDWI, rainfall, slope angle, and soil type are the critical landslides influencing factors along the highway.

Declarations

References

Ahmed B (2015) Landslide susceptibility mapping using multi-criteria evaluation techniques in Chittagong Metropolitan Area, Bangladesh. Landslides 12(6):1077–1095

Ahmed MF et al (2014) A regional level preliminary landslide susceptibility study of the upper Indus river basin. Eur J Remote Sens 47(1):343–373

Akgun A et al (2008) Landslide susceptibility mapping for a landslide-prone area (Findikli, NE of Turkey) by likelihood-frequency ratio and weighted linear combination models. Environ Geol 54(6):1127–1143

Ali S et al (2019) Landslide susceptibility mapping by using a geographic information system (GIS) along the China-Pakistan Economic Corridor (Karakoram Highway), Pakistan. Nat Hazards Earth Syst Sci 19(5):999–1022

Alimohammadlou Y et al (2014) Estimation of rainfall-induced landslides using ANN and fuzzy clustering methods: a case study in Saeen Slope, Azerbaijan province, Iran. CATENA 120:149–162

Anderson JR (1971) Land-use classification schemes. Photogramm Eng 37(4):379–387

Apurv T et al (2015) Impact of climate change on floods in the Brahmaputra basin using CMIP5 decadal predictions. J Hydrol 527:281–291

Arnoldus H (1980) An approximation of the rainfall factor in the universal soil loss equation. An approximation of the rainfall factor in the universal soil loss equation. Wiley, Chichester, pp 127–132

Ayalew L et al (2005) Landslides in Sado Island of Japan: Part II. GIS-based susceptibility mapping with comparisons of results from two methods and verifications. Eng Geol 81(4):432–445

Basharat M et al (2016) Landslide susceptibility mapping using GIS and weighted overlay method: a case study from NW Himalayas, Pakistan. Arabian J Geosci 9(4):1–19

Calligaris C et al (2013) First steps towards a landslide inventory map of the Central Karakoram National Park. Eur J Remote Sens 46(1):272–287

Carlson TN, Ripley DA (1997) On the relation between NDVI, fractional vegetation cover, and leaf area index. Remote Sens Environ 62(3):241–252

Cevik E, Topal T (2003) GIS-based landslide susceptibility mapping for a problematic segment of the natural gas pipeline, Hendek (Turkey). Environ Geol 44(8):949–962

Chen W et al (2016) Spatial prediction of landslide susceptibility using integrated frequency ratio with entropy and support vector machines by different kernel functions. Environ Earth Sci 75(20):1–15

Cui Y et al (2019) The cost of rapid and haphazard urbanization: lessons learned from the Freetown landslide disaster. Landslides 16(6):1167–1176

Dehnavi A et al (2015) A new hybrid model using step-wise weight assessment ratio analysis (SWARA) technique and adaptive neuro-fuzzy inference system (ANFIS) for regional landslide hazard assessment in Iran. CATENA 135:122–148

Demir G (2019) GIS-based landslide susceptibility mapping for a part of the North Anatolian Fault Zone between Reşadiye and Koyulhisar (Turkey). CATENA 183:104211

Ding M et al (2018) Surge-type glaciers in Karakoram Mountain and possible catastrophes alongside a portion of the Karakoram Highway. Nat Hazard 90(2):1017–1020

DiPietro JA, Pogue KR (2004) Tectonostratigraphic subdivisions of the Himalaya: a view from the west. Tectonics. https://doi.org/10.1029/2003TC001554

Ekumah B et al (2020) Geospatial assessment of ecosystem health of coastal urban wetlands in Ghana. Ocean Coast Manag 193:105226

Ercanoglu M, Gokceoglu C (2004) Use of fuzzy relations to produce landslide susceptibility map of a landslide prone area (West Black Sea Region, Turkey). Eng Geol 75(3–4):229–250

Feizizadeh B, Blaschke T (2011) Landslide risk assessment based on GIS multi-criteria evaluation: a case study in Bostan-Abad County, Iran. J Earth Sci Eng 1(1):66–77

Fell R et al (2008) Guidelines for landslide susceptibility, hazard and risk zoning for land-use planning. Eng Geol 102(3–4):99–111

Fressard M et al (2014) Which data for quantitative landslide susceptibility mapping at operational scale? Case study of the Pays d'Auge plateau hillslopes (Normandy, France). Nat Hazards Earth Syst Sci 14(3):569–588

Froude MJ, Petley DN (2018) Global fatal landslide occurrence from 2004 to 2016. Nat Hazards Earth Syst Sci 18(8):2161–2181

Goudie A et al (1984) The geomorphology of the Hunza valley, Karakoram mountains, Pakistan. In: The international Karakoram project. International conference

Greco R et al (2007) Logistic regression analysis in the evaluation of mass movements susceptibility: the Aspromonte case study, Calabria, Italy. Eng Geol 89(1–2):47–66

Guo Z et al (2017) Hazard assessment of potentially dangerous bodies within a cliff based on the Fuzzy-AHP method: a case study of the Mogao Grottoes, China. Bull Eng Geol Environ 76(3):1009–1020

Guzzetti F et al (1999) Landslide hazard evaluation: a review of current techniques and their application in a multi-scale study, Central Italy. Geomorphology 31(1–4):181–216

Hewitt K (1998) Catastrophic landslides and their effects on the Upper Indus streams, Karakoram Himalaya, northern Pakistan. Geomorphology 26(1–3):47–80

Hong H et al (2017) A hybrid fuzzy weight of evidence method in landslide susceptibility analysis on the Wuyuan area, China. Geomorphology 290:1–16

Hong H et al (2018) Improving the accuracy of landslide susceptibility model using a novel region-partitioning approach. Landslides 15(4):753–772

Horn BK (1981) Hill shading and the reflectance map. Proc IEEE 69(1):14–47

Jade S et al (2004) GPS measurements from the Ladakh Himalaya, India: preliminary tests of plate-like or continuous deformation in Tibet. Geol Soc Am Bull 116(11–12):1385–1391

Kamp U et al (2008) GIS-based landslide susceptibility mapping for the 2005 Kashmir earthquake region. Geomorphology 101(4):631–642

Kanwal S et al (2017) GIS based landslide susceptibility mapping of northern areas of Pakistan, a case study of Shigar and Shyok Basins". Geomat Nat Hazards Risk 8(2):348–366

Khan H et al (2019) Landslide susceptibility assessment using frequency ratio, a case study of northern Pakistan. Egypt J Remote Sens Space Sci 22(1):11–24

Kirschbaum D et al (2015) Spatial and temporal analysis of a global landslide catalog. Geomorphology 249:4–15

Lee S, Min K (2001) Statistical analysis of landslide susceptibility at Yongin, Korea. Environ Geol 40(9):1095–1113

Mandal B, Mandal S (2018) Analytical hierarchy process (AHP) based landslide susceptibility mapping of Lish river basin of eastern Darjeeling Himalaya, India. Adv Space Res 62(11):3114–3132

Mondal S, Maiti R (2013) Integrating the analytical hierarchy process (AHP) and the frequency ratio (FR) model in landslide susceptibility mapping of Shiv-khola watershed, Darjeeling Himalaya. Int J Disaster Risk Sci 4(4):200–212

Moosavi V, Niazi Y (2016) Development of hybrid wavelet packet-statistical models (WP-SM) for landslide susceptibility mapping. Landslides 13(1):97–114

Nascimento KRDS, Alencar MH (2016) Management of risks in natural disasters: a systematic review of the literature on NATECH events. J Loss Prev Process Ind 44:347–359

Oh H-J, Pradhan B (2011) Application of a neuro-fuzzy model to landslide-susceptibility mapping for shallow landslides in a tropical hilly area. Comput Geosci 37(9):1264–1276

Park S et al (2013) Landslide susceptibility mapping using frequency ratio, analytic hierarchy process, logistic regression, and artificial neural network methods at the Inje area, Korea. Environ Earth Sci 68(5):1443–1464

Paulín GL et al (2013) An overview of a GIS method for mapping and assessing landslide hazards. Landslide science and practice. Springer, Berlin, pp 379–385

Pavelsky TM, Smith LC (2008) RivWidth: a software tool for the calculation of river widths from remotely sensed imagery. IEEE Geosci Remote Sens Lett 5(1):70–73

Pourghasemi HR, Rossi M (2017) Landslide susceptibility modeling in a landslide prone area in Mazandarn Province, north of Iran: a comparison between GLM, GAM, MARS, and M-AHP methods. Theor Appl Climatol 130(1):609–633

Pourghasemi HR et al (2012) Application of fuzzy logic and analytical hierarchy process (AHP) to landslide susceptibility mapping at Haraz watershed, Iran. Nat Hazard 63(2):965–996

Pourghasemi HR et al (2016) A comparative assessment of prediction capabilities of modified analytical hierarchy process (M-AHP)

and Mamdani fuzzy logic models using Netcad-GIS for forest fire susceptibility mapping. Geomat Nat Hazards Risk 7(2):861–885

Pradhan B, Lee S (2009) Landslide risk analysis using artificial neural network model focussing on different training sites. Int J Phys Sci 4(1):1–15

Pradhan B et al (2010) Weights-of-evidence model applied to landslide susceptibility mapping in a tropical hilly area. Geomat Nat Hazards Risk 1(3):199–223

Pradhan B et al (2017) Performance evaluation and sensitivity analysis of expert-based, statistical, machine learning, and hybrid models for producing landslide susceptibility maps. Laser scanning applications landslide assessment. Springer, Cham, pp 193–232

Ray R, De Smedt F (2009) Slope stability analysis on a regional scale using GIS: a case study from Dhading, Nepal. Environ Geol 57(7):1603–1611

Refice A, Capolongo D (2002) Probabilistic modeling of uncertainties in earthquake-induced landslide hazard assessment. Comput Geosci 28(6):735–749

Reichenbach P et al (2014) The influence of land use change on landslide susceptibility zonation: the Briga catchment test site (Messina, Italy). Environ Manag 54(6):1372–1384

Restrepo C, Alvarez N (2006) Landslides and their contribution to land-cover change in the mountains of Mexico and Central America 1. Biotropica 38(4):446–457

Saaty RW (1987) The analytic hierarchy process—what it is and how it is used. Math Model 9(3–5):161–176

Saaty TL (1990) How to make a decision: the analytic hierarchy process. Eur J Oper Res 48(1):9–26

Saaty TL (2008) Decision making with the analytic hierarchy process. Int J Serv Sci 1(1):83–98

Saha S et al (2019) Identification of soil erosion-susceptible areas using fuzzy logic and analytical hierarchy process modeling in an agricultural watershed of Burdwan district, India. Environ Earth Sci 78(23):1–18

Samia J et al (2017) Characterization and quantification of path dependency in landslide susceptibility. Geomorphology 292:16–24

Schilirò L et al (2016) Prediction of shallow landslide occurrence: validation of a physically-based approach through a real case study. Sci Total Environ 569:134–144

Shahabi H, Hashim M (2015) Landslide susceptibility mapping using GIS-based statistical models and remote sensing data in tropical environment. Sci Rep 5(1):1–15

Shahabi H et al (2012) Application of satellite remote sensing for detailed landslide inventories using frequency ratio model and GIS. Int J Comput Sci 9:108–117

Shahabi H et al (2015) Remote sensing and GIS-based landslide susceptibility mapping using frequency ratio, logistic regression, and fuzzy logic methods at the central Zab basin, Iran. Environ Earth Sci 73(12):8647–8668

Shahri AA et al (2019) Landslide susceptibility hazard map in southwest Sweden using artificial neural network. CATENA 183:104225

Sidle R, Ochiai H (2006) Processes, prediction, and land use. Water resources monograph. American Geophysical Union, Washington

Suh J et al (2011) National-scale assessment of landslide susceptibility to rank the vulnerability to failure of rock-cut slopes along expressways in Korea. Environ Earth Sci 63(3):619–632

Sujatha ER et al (2014) Assessing landslide susceptibility using Bayesian probability-based weight of evidence model. Bull Eng Geol Environ 73(1):147–161

Umar Z et al (2014) Earthquake induced landslide susceptibility mapping using an integrated ensemble frequency ratio and logistic regression models in West Sumatera Province, Indonesia. CATENA 118:124–135

Van Westen C et al (2006) Landslide hazard and risk zonation—why is it still so difficult? Bull Eng Geol Environ 65(2):167–184

Wang Q et al (2015) GIS-based assessment of landslide susceptibility using certainty factor and index of entropy models for the Qianyang County of Baoji city, China. J Earth Syst Sci 124(7):1399–1415

Wang Q et al (2016) Landslide susceptibility mapping at Gongliu county, China using artificial neural network and weight of evidence models. Geosci J 20(5):705–718

Weirich F, Blesius L (2007) Comparison of satellite and air photo based landslide susceptibility maps. Geomorphology 87(4):352–364

Wentworth CK (1930) A simplified method of determining the average slope of land surfaces. Am J Sci 5(117):184–194

Wu Y et al (2016) Application of analytic hierarchy process model for landslide susceptibility mapping in the Gangu County, Gansu Province, China. Environ Earth Sci 75(5):422

Xu J et al (2016) Natural disasters and social conflict: a systematic literature review. Int J Disaster Risk Reduct 17:38–48

Yalcin A (2008) GIS-based landslide susceptibility mapping using analytical hierarchy process and bivariate statistics in Ardesen (Turkey): comparisons of results and confirmations. CATENA 72(1):1–12

Yan F et al (2019) A novel hybrid approach for landslide susceptibility mapping integrating analytical hierarchy process and normalized frequency ratio methods with the cloud model. Geomorphology 327:170–187

Zeitler PK (1985) Cooling history of the NW Himalaya, Pakistan. Tectonics 4(1):127–151

Zevenbergen LW, Thorne CR (1987) Quantitative analysis of land surface topography. Earth Surf Process Landf 12(1):47–56

Zhiquan Y et al (2016) Types and space distribution characteristics of debris flow disasters along China–Pakistan Highway. Electron J Geotech Eng 21:191–200